

Self-organization in Navier-Stokes turbulence

Jacques Lewalle
Syracuse University
jlewall@syr.edu

Fluid turbulence is undoubtedly a complex phenomenon, but the relation between the fundamental laws and the emergence of large-scale coherent eddies from differential interactions in a random background has remained elusive. Such a connection is attempted in this paper. The key analytical step is to express the Navier-Stokes equations in the Hermitian wavelet representation, which adds one independent spectral variable to the spatial description at any instant. In this expanded representation, the equations reduce naturally to a form consistent with pairwise nonlinear interactions governed by known kernels. The emergence of strong eddies from a random background, and their eventual breakdown, are illustrated by a 2-dimensional simulation.

1 Introduction

Fluid turbulence is, with various attributions (see e.g. [10], p.3), ‘... *the last great unsolved problem of classical physics*’. One might accept as likely that it belongs in the new field of dynamics of complex systems, which generate ‘complicated’ behavior from simple inputs. Nicolis & Prigogine [14] focused on chaotic dynamics and generic instabilities as relevant to complexity in the mathematical sciences, but no theory of turbulence has yet evolved on these premises. A complex system usually includes many interacting parts, resulting in cooperative (rather than merely collective) behavior (Bar-Yam [2]). Also significant is the difference between fine- and coarse-grained descriptions, which introduces the concept of scale. Scaling properties are usually statistical, but the ergodic assumption is not expected to hold for organized structures. Badii & Politi [1] emphasize a *hierarchy* of parts, interactions and scaling as relevant to complex physical systems. For generic parts $Y(x)$, the (arguably) simplest

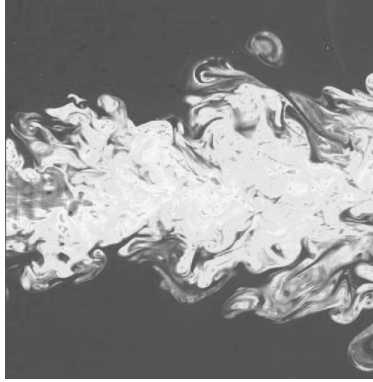


Figure 1: longitudinal section of a turbulent jet, obtained by laser induced fluorescence, courtesy of C. Fukushima and J. Westerveel (Technical University of Delft, the Netherlands) and of efluids.com. The dye concentration reflects the cumulative history of mixing as the jet develops from left to right.

evolution equation associated with complex behavior is

$$\frac{dY}{dt} = A * (YY) \quad (1)$$

The local kernel $A(x)$ is convolved (asterisk) with nonlinear expressions, resulting in interactions with nearby parts only. Based on such a lattice model, Hansen & Tabeling [9] illustrated the emergence of eddies (see also [3]), paving the way for a more fundamental study based on exact equations.

This highlights the need to identify relevant ‘parts’ in the turbulence problem. Among the contenders, Fourier modes are unsatisfactory in spite of significant successes, because they conceal the localized nature of eddies. With the Karhunen-Loeve eigenmodes, success is most definite in systems where few modes are active. Finally, vortices have been effective in two-dimensional turbulence [4, 7], but less so in three-dimensional flows. Each of these fundamental ‘parts’ captures some important feature of turbulence while others remain elusive. Badii & Politi [1] point out that ‘...*The concept of complexity is closely related to that of understanding...*’. In the turbulence problem, our lack of understanding is epitomized by the poor match between established descriptive concepts (e.g. eddies) and analytical formulations.

The example shown on Fig. 1 illustrates the presence of large and small scale eddies in a section of a jet. As instabilities break up the large eddies into smaller ones, energy cascades from large to smaller scale in an intermittent process. The spatial and spectral distribution and variable intensity of eddies, and their embedding patterns, is the core of the turbulence problem.

2 Basic equations

2.1 Fundamental laws

Fluid turbulence falls within the scope of classical dynamics (Newton). The extension to continua by Euler introduced the nonlinearity essential to the existence of turbulence. Then, Cauchy showed that tangential (viscous) stresses must be added to Euler's isotropic pressure p . The result for the simplest case (Newtonian incompressible fluids) is due to Navier and Stokes ¹ :

$$\partial_t u_i + u_j \partial_j u_i = -\frac{1}{\rho} \partial_i p + \nu \partial_{jj}^2 u_i. \quad (2)$$

Here ρ is the fluid's density and ν its viscosity. Eq.(2) constitutes the inescapable mathematical and physical basis for turbulence dynamics. Since it has three components, and four unknowns u_i and p , it must be supplemented by mass conservation $\partial_i u_i = 0$. Hence, we have a system of four field equations for velocity and pressure at each point. The elimination of pressure has been done traditionally in Fourier space (see e.g. [13]) or through the use of vorticity $\underline{\omega} = \nabla \times \underline{U}$. This paper is based on a new alternative.

Let us define flexion as the Laplacian of velocity $\alpha_i = \partial_{jj}^2 u_i$. The application of the Laplacian to Eq.(2) and simple substitutions give

$$\partial_t \alpha_i - \nu \partial_{jj}^2 \alpha_i = \partial_{ijk}^3 (u_j u_k) - \partial_{jkk}^3 (u_i u_j) \quad (3)$$

The left side of the Eq.(3) shows the familiar diffusion equation; the cost of the elimination of pressure is seen on the right side, with triple derivatives of the nonlinear terms somehow responsible for the phenomena of turbulence. Assuming a solution α_i for the flexion vector, the velocity field can be reconstructed using the Biot-Savart equation (3-D version shown here)

$$u_i = -\frac{1}{4\pi} \int \frac{\alpha_i(x')}{|x - x'|} dV'. \quad (4)$$

2.2 Wavelet transforms and reformulation

Eq.(3) is more familiar in its Fourier representation [13]. Then, the spectral decomposition obscures the spatial intermittence (i.e. the presence of organized motion at each scale), whereas in the spatial representation, eddies of all scales are superposed. In the wavelet representation [5, 6], we can select the point of compromise between spectral and spatial accuracy to suit our own purposes.

¹For notations, the components of the velocity vector \underline{U} will be indexed as u_i , with $i = 1 \dots N$ in N dimensions. N will have the default value 3 in this paper; use of $N = 2$ will be clear from the context. The total or material time derivative $\frac{d}{dt}$, the local or apparent time derivative $\frac{\partial}{\partial t}$, and the spatial derivatives $\frac{\partial}{\partial x_i}$ will be abbreviated respectively as d_t , ∂_t and ∂_i . Second and higher-order derivatives will follow the notational pattern $\partial_i \partial_j = \partial_{ij}^2$. Summation over repeated indices is assumed. Depending on context, x will stand either for one Cartesian coordinate, as in (x, y) , or for the generic coordinate vector \underline{x} .

Wavelets [5, 6] can be discrete (orthogonal) or continuous (redundant). Either way, when used in integral transforms, they meet the requirements of the existence of an inverse transform (no loss of information) and of Parseval's theorem (L^2 normalization). A variant of the Mexican hat continuous wavelet is used here.

Based on the normalized N -dimensional Gaussian filter $F_s(x) = e^{-x^2/4s} / (2\sqrt{\pi s})^N$ of scale s (note that s has dimensions L^2), the wavelet transform of a velocity component $u_i(x)$ at any time t is identical to filtered flexion

$$\tilde{u}_i(x, s, t) = \nabla^2 F_s * u_i(x, t) = \psi_s(x) * u_i(x, t) = F_s * \alpha_i(x, t) = F_s * \tilde{u}_i(x, 0, t), \quad (5)$$

where the asterisk denotes spatial convolution². While, in general [5, 6], the inverse wavelet transform includes a convolution, in this case it takes the particularly simple form [11]:

$$u_i(x, t) = - \int_0^\infty (s \tilde{u}_i(x, s, t)) \frac{ds}{s} = - \int_0^\infty F_s * \alpha_i ds. \quad (6)$$

The mapping from flexion to velocity is equivalent to Eq.(4), but Eq.(6) is valid for any space dimension N [12]. Thus the quantity $s\tilde{u}_i$ appears as a natural building block, with superposition over all (logarithmic) scales to reconstruct the field u_i or (when squared) its energy density. For a 1-dimensional signal, the distribution of energy is shown on Fig. 2. The lumping of the energy density into quasi-discrete objects in the $(x - s)$ -space suggests that the property $s\tilde{u}_i$ is one possible analytical tool to capture eddies. In contrast to the lumpy $s\tilde{u}_i$, the wavelet coefficients \tilde{u}_i show a gradual relaxation from $s = 0$ toward larger scales, and increasing the wavelet scale corresponds to coarse-graining of the flexion field.

The equation governing the evolution of the wavelet coefficients is obtained by filtering of Eq.(3), yielding

$$(\partial_t - \nu \partial_{jj}^2) \tilde{u}_i = \partial_{ijk}^3 F_s * (u_j u_k) - \partial_{jkk}^3 F_s * (u_i u_j) = F_{ijk} * (u_j u_k) - F_{jkk} * (u_i u_j) \quad (7)$$

The definition of F_{ijk} is self-explanatory. The nonlinear terms (right side) include the convolution with a known localized interaction kernel F_{ijk} , as in the generic model Eq.(1). However, the kernel acts not on the wavelet coefficient \tilde{u}_i , but, through the inverse transform formula, on wavelet coefficients at all scales, obtained by filtering of the fine-grained coefficient. It is sufficient to solve a fine-grained version (small s) of this equation, with all larger scale (coarser grained) solutions implied by filtering.

3 A 2-D periodic simulation

The spectral flexion equation (7) describes three distinct phenomena that combine into turbulence: diffusion, spatial organization and spectral exchanges.

²The numerical coefficients and specific scaling reflect the particular definition of the wavelet transform adopted here; alternatives can be found e.g. in [5, 15], and it is important to use an internally consistent set of relations. The present selection was derived in [11].

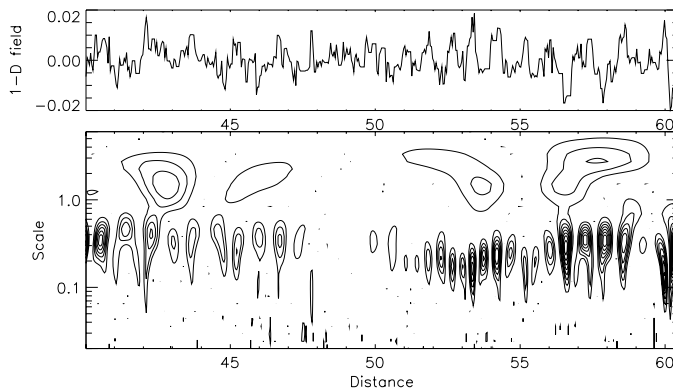


Figure 2: Local spectral energy density contours for the signal shown in the upper box; units of space and scale match, but are otherwise arbitrary.

Simplifying the problem to two dimensions on a 32^2 -grid, we can use u and v components in the cartesian directions x and y , respectively, rather than the generic indices. This gives

$$(\partial_t - \nu \partial_{jj}^2) \tilde{u} = [F_{xxy} * (uv) + F_{xyy} * (vv) - F_{xyy} * (uu) - F_{yyy} * (uv)] \quad (8)$$

and

$$(\partial_t - \nu \partial_{jj}^2) \tilde{v} = [F_{xxy} * (uu) + F_{xyy} * (uv) - F_{xxx} * (uv) - F_{xxy} * (vv)]. \quad (9)$$

The interaction kernels F_{ijk} can be constructed as products of factors in the cartesian directions; each factor is an approximation of derivatives of a bell-shaped curve. The fourth-order central-difference coefficients were adopted as a model. The resulting discrete and continuous interaction kernels are in excellent qualitative and quantitative agreement. Note that, in 2 dimensions, the 3 derivatives must arrange themselves so that an even-ordered derivative applies in one direction (and the kernel is symmetric in that direction) and an odd-ordered derivative applies in the other direction (with anti-symmetry of the kernel). Because each kernel contains derivatives in at least one direction, its average is zero, so that the dynamics conserve the total amount of \tilde{u} and \tilde{v} in the system, and merely rearrange them spatially.

3.1 2-D velocity field reconstruction

Velocity field reconstruction from Eq.(6) is necessary to evaluate the nonlinear terms. In addition, vorticity is a useful property for the graphical interpretation

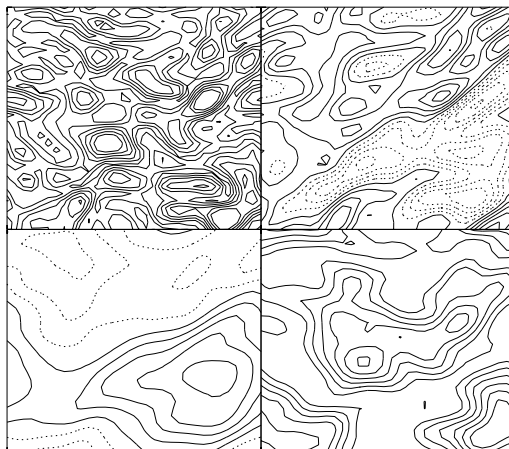


Figure 3: Clockwise from top left: flexion, vorticity, velocity and streamfunction magnitudes obtained from the initial (incompressible) flexion components. Each map has unit variance, contour lines from -3 to +3 by intervals of 0.5, dotted lines for negative values.

of 2-D flows, because only the component normal to the plane of the flow is non-zero. The relations between the streamfunction (defined below), velocity, vorticity and flexion also provide accuracy diagnostics, and are summarized next.

The streamfunction $\psi(x, y)$ is a function such that the velocity components u and v can be obtained from the relations $u = -\partial_y\psi$ and $v = \partial_x\psi$. For any sufficiently smooth such function ψ , the continuity equation is automatically satisfied. In 2-D flows, the vorticity vector has only one component $\omega = \partial_x v - \partial_y u$ normal to the plane of the flow. Then, the flexion components are given by $\alpha_x = \nabla^2 u = -\partial_y \omega$ and $\alpha_y = \nabla^2 v = \partial_x \omega$. It is a simple matter to verify that $\omega = \nabla^2 \psi$ and $\alpha_i = \nabla^2 u_i$. This classical sequence can be inverted from flexion to velocity (Eq.6) to vorticity to streamfunction, the latter resulting from the inversion of the Laplacian $\psi = -\int_0^\infty F_s * \omega ds$ similar to Eq.(6).

The initial conditions to be used below served as an example of the reconstruction technique and accuracy check. They were generated by assigning random numbers to the grid values of the streamfunction and filtering. The velocity, vorticity and flexion fields were then calculated by central differences. Then, starting with the flexion fields, the other properties were reconstructed as described above, and the values compared to the originals. Errors of the order of 2% were observed. After normalization of the variance for each map, the results are plotted on Fig. 3. The vorticity map will be used as we track the evolution of the field under Navier-Stokes dynamics. Two additional quantities provide useful diagnostics. Given a wavelet coefficient \tilde{u} , a scale-dependent local Reynolds number, or eddy Reynolds number, can be defined as $Re_s = \frac{s^{3/2}\tilde{u}}{\nu}$. Similarly, the eddy inverse time scale (turnover rate) is given by $f = s^{1/2}\tilde{u} = \frac{Re_s\nu}{s}$.

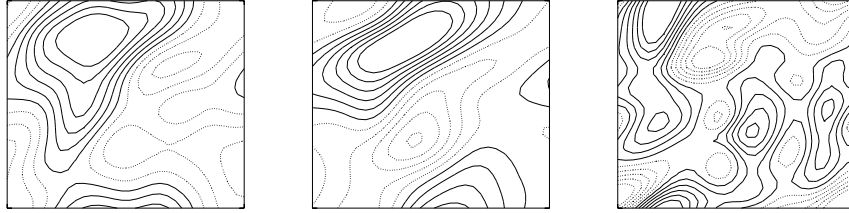


Figure 4: The evolution of normalized vorticity shown on Fig. 3 at dimensionless times 0.25, 0.4 and 0.5. Contour levels range from -2 to +2.

4 Simulation results and discussion

The evolution in Eqs. (8) and (9) was tracked with a second-order Runge-Kutta scheme. The results are independent of the time increment. The supremum of the inverse time scale is used to adjust the time-step to current conditions. Overall time is non-dimensionalized by the initial time scale. An initial eddy Reynolds number (supremum) of 150 was used. Results at times 0.25, 0.4 and 0.5 are shown on Fig. 4. In the first phase of evolution, the field organizes itself into a large-scale vorticity distribution. Little convection is observed in the poorly organized field. The maximum eddy Re_s , distinct from the traditional mean Re , increases with the dominant scale to approximately 2000, a twelve-fold increase. In the second phase of evolution, the large eddies break down into smaller eddies again. Simulations on larger grids, and in 3-D, will be necessary to diagnose the differences in correlations and scaling relations between the initial (unstructured) eddy distribution and the later outcome of a cascade process. This is the subject of current work by several groups (e.g. Farge, private communication, 2002).

A century-and-a-quarter of efforts have yielded remarkably few exact results and no physical theory of Navier-Stokes turbulence. The source of difficulty is that the basic empirical concepts of turbulence (scaling, intermittence, eddies, cascade) are poorly expressed by the traditional analytical tools. The wavelet representation captures the local spectral behavior and translates it into a lumpy distribution of magnitude and energy. The Mexican hat transform is identical to filtered flexion and thus related to vorticity as well. Filtering, of course, expresses the fine- vs. coarse-graining of renormalization approaches. With these tools, the Navier-Stokes dynamics for the wavelet coefficients are local and non-differential in space, and the nonlinear interactions are governed by fixed known localized kernels and involve local wavelet coefficients at all scales. On this basis, the wavelet representation of the Navier-Stokes equations is unusually promising.

Bibliography

- [1] BADI, Remo and A. POLITI, *Complexity: Hierarchical structures and scaling in physics*, Cambridge Univ. Press (1997).
- [2] BAR-YAM, Yaneer, *Dynamics of complex systems*, Perseus Books (1997).
- [3] BOHR, Tomas, M.H. JENSEN, G. PALADIN and A. VULPIANI, *Dynamical Systems Approach to Turbulence*, Cambridge Univ. Press (1998).
- [4] CHORIN, Alexander J., *Vorticity and turbulence*, Springer Verlag (1994).
- [5] DAUBECHIES, Ingrid, *Ten Lectures on Wavelets*, S.I.A.M. (1992).
- [6] FARGE, Marie, “Wavelet transforms and their applications to turbulence”, *Ann. Rev. Fluid Mech.* **24** (1992), 395-457.
- [7] FARGE, Marie, K. SCHNEIDER and N. KEVLAHAN, “Non-gaussianity and coherent vortex simulation for two-dimensional turbulence using an adaptive orthogonal wavelet basis”, *Phys. Fluids* **11** (1999), 2187–2201.
- [8] FRISCH, Uriel, *Turbulence: the legacy of A.N. Kolmogorov*, Cambridge U. Press (1995).
- [9] HANSEN, A.E., and P. TABELING, “Coherent structures in two-dimensional decaying turbulence”, *Nonlinearity* **13** (2000), C1-C3.
- [10] HOLMES, Philip, J.L. LUMLEY and G. BERKOOZ, *Turbulence, coherent structures, dynamical systems and symmetry*, Cambridge U. Press (1996).
- [11] LEWALLE, Jacques, “Formal improvements in the solution of the wavelet-transformed Poisson and diffusion equations”, *J. Math. Phys.* **39** (1998), 4119–4128.
- [12] LEWALLE, Jacques, “A filtering and wavelet formulation for incompressible turbulence”, *J. Turbulence* **1** (2000), 004, 1–16.
- [13] McCOMB, W.D., *The Physics of Fluid Turbulence*, Clarendon Press (1990).
- [14] NICOLIS, Gregoire, and I. PRIGOGINE, *Exploring complexity*, W.H. Freeman and Co. (New York) (1989).
- [15] PERRIER, Valérie, and C. BASDEVANT, “Besov norms in terms of the continuous wavelet transform. Application to structure functions”, *Math. Models and Methods in Appl. Sciences* **6** (1996), 649–664.